Journal of Proteomics 192 (2019) 267–279

Contents lists available at ScienceDirect

Journal of Proteomics

journal homepage: www.elsevier.com/locate/jprot

Dehydration-induced proteomic landscape of mitochondria in chickpea reveals large-scale coordination of key biological processes

Dipak Gayen[a,1], Saurabh Gayali[a,1], Pragya Barua[a], Nilesh Vikram Lande[a], Swati Varshney[b], Shantanu Sengupta[b], Subhra Chakraborty[a], Niranjan Chakraborty[a,*]

[a] National Institute of Plant Genome Research, Jawaharlal Nehru University Campus, Aruna, Asaf Ali Marg, New Delhi, India
[b] CSIR-Institute of Genomics and Integrative Biology, Mathura Road, New Delhi, India

ARTICLE INFO

Keywords:
Cell defense
Dehydration
Cultivated legume
Metabolic alterations
Mitochondrial proteins
Proteomic landscape

ABSTRACT

Mitochondria play crucial roles in regulating multiple biological processes particularly electron transfer and energy metabolism in eukaryotic cells. Exposure to water-deficit or dehydration may affect mitochondrial function, and dehydration response may dictate cell fate decisions. iTRAQ-based quantitative proteome of a winter legume, chickpea, demonstrated the central metabolic alterations in mitochondria, presumably involved in dehydration adaptation. Three-week-old chickpea seedlings were subjected to progressive dehydration and the magnitude of dehydration-induced compensatory physiological responses was monitored in terms of physicochemical characteristics and mitochondrial architecture. The proteomics analysis led to the identification of 40 dehydration-responsive proteins whose expressions were significantly modulated by dehydration. The differentially expressed proteins were implicated in different metabolic processes, with obvious functional tendencies toward purine-thiamine metabolic network, pathways of carbon fixation and oxidative phosphorylation. The linearity of dehydration-induced proteome alteration was examined with transcript abundance of randomly selected candidates under multivariate stress conditions. The differentially regulated proteins were validated through sequence analysis. An extensive sequence based localization prediction revealed > 62.5% proteins to be mitochondrial resident by, at least, one prediction algorithm. The results altogether provide intriguing insights into the dehydration-responsive metabolic pathways and useful clues to identify crucial proteins linked to stress tolerance.

Biological significance: Investigation on plant mitochondrial proteome is of significance because it would allow a better understanding of mitochondrial function in plant adaptation to stress. Mitochondria are the unique organelles, which play a crucial role in energy metabolism and cellular homeostasis, particularly when exposed to stress conditions. Chickpea is one of the cultivated winter legumes, which enriches soil nitrogen and has very low water footprint and thus contributes to fortification of sustainable agriculture. We therefore examined the dehydration-responsive mitochondrial proteome landscape of chickpea and queried whether molecular interplay of mitochondrial proteins modulate dehydration tolerance. A total of 40 dehydration-induced mitochondrial proteins were identified, predicted to be involved in key metabolic processes. Our future efforts would focus on understanding both posttranslational modification and processing for comprehensive characterization of mitochondrial protein function. This approach will facilitate mining of more biomarkers linked to the tolerance trait and contribute to crop adaptation to climate change.

1. Introduction

Plant productivity has become a major challenge, especially under stress conditions, to meet the global food demand. Water-deficit or dehydration affects crop yield more than any other environmental stress worldwide, particularly in rainfed areas [1–3]. The recent trend of climate change in response to global warming is likely to cause dehydration more severe than it has been in the past decades. While dehydration restricts growth and development of plants throughout their lifecycle, the early vegetative growth stages are more prone to such stress [4]. To date, most studies on water-deficit stress have focused on differential gene expression, especially in model plants [5]. But due to

* Corresponding author at: National Institute of Plant Genome Research, Jawaharlal Nehru University Campus, Aruna Asaf Ali Marg, New Delhi 110067, India.
E-mail address: nchakraborty@nipgr.ac.in (N. Chakraborty).
[1] These authors contributed equally to this work.

https://doi.org/10.1016/j.jprot.2018.09.008
Received 9 May 2018; Received in revised form 9 August 2018; Accepted 11 September 2018
Available online 19 September 2018
1874-3919/ © 2018 Elsevier B.V. All rights reserved.

high levels of genetic divergence between the model plants and crops, the extrapolation of information may be difficult and may lack reliability. Further, while such studies have evaluated dehydration-induced transcriptional activation and expression of large number of genes [6], an accurate knowledge of the identity of their constituent proteins, and site of action are still lacking.

Spatial partitioning of cellular processes is a fundamental feature of life, which facilitates multiple parallel pathways to occur in specialized subunits, the organelles. Therefore, the knowledge of organelle proteome is of paramount biological importance, and is critical to understanding of cellular biology. The organelle proteomics research in yeast and mammals is quite advanced, while plant organelle proteomics is lagging far behind, and constrained due to inter-plant, inter-tissue complexity, and difficulties in isolation of intact organelles [7]. The recent technological advances in proteomics have contributed to an increasing understanding of the cellular organelles and their functions and more importantly, how their protein components impact to plant development and stress tolerance [8].

The mitochondria are one of the most crucial cellular organelles contributing to generation of metabolic energy. They are universally distributed in bacteria and archaebacterial, animal and plant cells, where ATP is synthesized through oxidative phosphorylation of organic acids [9,10]. Due to the complex mechanism of actions, mitochondria are regarded as “signaling hubs” of cell [11]. Much interest in mitochondrial research resurged after being implicated in a wide variety of functions including intracellular signaling and cell defense. In plants, the mitochondrial respiration plays positive role in development, metabolism, stress response and programmed cell death [12,13]. The number of proteins encoded by mitochondrial genome ranges from 25 to 40, whereas the rests are transported from nucleus and other organelles [14]. Under stress conditions, mitochondria integrate the stress-induced signals and translate them into the energy-deficiency process, and balance the metabolic process [15]. Mitochondria also accelerate nuclear gene expression and dictate cell fate decision. Oxidative stress has long been implicated in mitochondrial dysfunction and the role of reactive oxygen species (ROS) in signal transduction has been elucidated in pea [16,17]. Late-embryogenesis abundant (LEA) proteins play important role in desiccation tolerance by stabilizing mitochondrial matrix of pea [18–21] and Arabidopsis [22,23]. The structure-function relationship and physicochemical properties of most LEA proteins have been well established [24]. Mitochondria has crucial role in seed development where majority of proteins were predominately involved in energy metabolism, protein transport, and protein folding, besides ROS detoxification [25]. In a classical study, chilling stress-responsive soybean mitochondrial proteome was shown to revamp the TCA cycle, oxidative phosphorylation complex and mitochondrial metabolism [26]. Furthermore, the pathways related to γ-amino butyrate shunt and TCA cycle were shown to be activated, and reprogrammed in soybean seedlings when exposed to flooding stress [27]. Yet another study demonstrated the involvement of mitochondrial ROS under flooding stress [28]. The high temperature stress-induced mitochondrial proteome of cauliflower curd revealed upregulation of mitochondrial complexome, linked to mitochondrial biogenesis [29]. A comprehensive study of potato tuber proteome identified a large number of mitochondrial proteins predominantly involved in metabolism, electron transport chain, respiration and posttranslational regulation [30]. A recent study on the complexome profiling identified 1359 unique proteins demonstrating protein-protein interaction in mitochondria complex [31].

To obtain a global overview of how mitochondria respond to dehydration, we aimed to define the dehydration-responsive mitochondrial proteome of chickpea, a winter crop which have evolved into growing in water-deficit conditions. We developed a reference proteome map followed by a dehydration-responsive proteome using isobaric tagging of mitochondrial proteins. The proteomic landscape revealed 40 dehydration-responsive proteins (DRPs), presumably involved in metabolic and cellular processes, and cell defense. The mitochondrial proteome dynamics may provide new insights into the underlying mechanism of stress adaptation in plants. These results may also be useful to guide effective genetic manipulation of cultivated chickpea to increase legume productivity.

2. Materials and methods

2.1. Seedling growth and development, and dehydration treatment

Chickpea (*Cicer arietinum* L. cv. JG-62) seeds were imbibed overnight in water and germinated in pots (18 cm diameter; capacity: 1.5 L) containing mixture of soil and soilrite (2:1, *w*/w) under fluorescent white light (300 μmol m^{-2} s^{-1}, 16 h photoperiod) at 25 ± 2 °C and 50 ± 5% relative humidity. Each pot was planted with 10 seedlings. For physicochemical analysis, three-week-old seedlings were subjected to dehydration by withholding water, and the aerial parts were harvested up to 144 h. Dehydration was imposed on 22nd day and tissues were harvested from unstressed as well as treated samples on 26th day implicating 72 h dehydration in treated samples. In a separate experiment, seedlings were subjected to other stresses by foliar spray with ABA (100 μM), methyl viologen (100 μM), jasmonic acid (100 μM) and ethylene (0.5 μM). The aerial tissues from 10 to 12 pots were harvested and pooled to reduce biological variation within each time point [32]. The harvested tissues were snap frozen in liquid nitrogen followed by storage at −80 °C until further use.

2.2. Ultrastructural analysis of mitochondria

Intact mitochondria were visualized by transmission electron microscopy (TEM) as described earlier [33]. Unstressed control and dehydrated leaves were harvested and quickly transferred to fixing solution, and kept overnight at room temperature. The samples were further processed to create resin blocks, which were sectioned using a Leica EM UC6 ultramicrotome (Leica Microsystems, Wetzlar, Germany). The sections were mounted on copper coated grids (TAAB, Berkshire, UK) and viewed using a cryo-transmission electron microscope JEM-2100F (JEOL, Tokyo, Japan).

2.3. Isolation of intact mitochondria and extraction of proteins

Intact mitochondria were isolated by the methods described earlier [30,34] with few modifications. Approximately, 50 g leaf-tissues were ground into powder with liquid nitrogen in a prechilled mortar and homogenized in 300 mL ice cold extraction buffer [0.3 M sucrose, 25 mM tetrasodium pyrophosphate, 2 mM EDTA, 10 mM KH_2PO_4, 1% (*w*/*v*) PVP-40 and 1% (w/v) BSA, pH 7.5]. The cell debris were removed from the homogenate by filtration through two layers of miracloth (Calbiochem, USA) and centrifuged at 1100*g* for 5 min at 4 °C. The supernatant was centrifuged at 18000*g* for 20 min and the pellet was suspended in wash buffer (0.3 M manitol, 10 mM TES and 0.1% BSA, pH 7.5), and retrieved by centrifugation. The pellet was dissolved in 1 mL wash buffer using a paintbrush, and intact mitochondria were recovered from Percoll gradient by centrifugation at 18000*g* for 60 min. The intact mitochondria were stained by Rhodamine-123 (10 μg/mL) for 30 min and washed three times with phosphate-buffered saline (PBS). The mitochondria were viewed using a TCS SP5 microscope (Leica Microsystems, Wetzlar, Germany) at 507 nm excitation and 529 nm emission.

Mitochondrial proteins were extracted by treatment with chilled acetone by storing overnight at −80 °C and precipitated by centrifugation at 20000*g* for 15 min. The protein pellet was resuspended in 7 M urea using water-bath sonicator. The urea was replaced from the protein samples by 0.5 M TEAB using 3-kDa column. The concentration of protein was determined by BCA protein assay (Thermo Fisher Scientific, USA).

2.4. Immunoblot analysis

Aliquots containing 50 μg of proteins were resolved onto SDS-PAGE (12.5%), followed by electrotransfer onto nitrocellulose membrane (PVDF, Milipore) for 2 h at 150 mA after activation with methanol. The membranes were blocked with 3% BSA in PBS and 0.1% Tween-20 for 2 h at room temperature. The blots were incubated independently with the primary antibodies [anti-LHC II (light harvesting complex II, Agrisera A S01 003), anti-TOC 75 (chloroplast outer envelope membrane translocon complex, Agrisera A S06 150), anti-Cox II (cytochrome oxidase II, Agrisera A S04 053A) and anti-Rubisco (RbcL, Agrisera AS03 037)] as per manufacturer's instructions. Next, the blots were washed three times for 10 min each with PBS containing 0.1% Tween-20 and incubated with HRP-conjugated secondary antibody for 2 h. Immunodetection was done using Clarity Western ECL Substrate (Bio-Rad Laboratories).

2.5. Purity assessment of mitochondrial proteins

The cytoplasmic contamination in the isolated mitochondrial fraction was examined by measuring the activity of UGPase [35]. Furthermore, integrity of the mitochondrial fraction was confirmed by estimation of COX activity in the presence/absence of detergent n-dodecyl β-D-maltoside [36].

2.6. Mitochondrial ATP measurement

ATP content was measured by luciferase-based assay as described previously [37]. ATP was isolated from intact mitochondria (500 μg) by 10% TCA and centrifuged at 10,000 ×*g* for 5 min at 4 °C. The supernatant was neutralized with 10 N KOH followed by centrifugation at 10,000 ×*g* for 5 min at 4 °C. The neutralized supernatant was used for measurement of ATP content by ATP determination kit (Molecular Probes).

2.7. Estimation of respiratory O_2 consumption

The respiratory O_2 consumption of mitochondria was measured using single-channel free radical analyzer (TBR 1025, World Precision Instruments, USA) as previously described [38].

2.8. Protein digestion and iTRAQ-labeling

Enriched mitochondrial fractions were buffer exchanged with 100 mM TEAB using a 3 kDa cut off column. Next, 60 μg proteins were reduced and alkylated as per manufacturer's instructions followed by in-solution trypsin digestion (1:10 enzyme-to-substrate ratio) at 37 °C for 16 h. The tryptic peptides were labelled by iTRAQ 4-plex kit (AB Sciex, Foster City, CA). The peptides from unstressed control and treated samples were labelled in replicates with 114, 115 and 116 and 117 iTRAQ tags, respectively. After labeling, the samples were pooled and dried in speed vacuum at 30 °C. The dried peptides were reconstituted in 1 mL buffer A (8 mM ammonium formate, 30% (*v*/v) ACN and 0.1% formic acid, pH 2.9) and applied to strong cation exchange (SCX) chromatography (SCX cartridge: 5 μm beads with 300 Å pores). The samples were fractionated using a step gradient of increasing concentrations of ammonium formate [30, 50, 70, 100, 125, 150 and 250 mM ammonium formate, 30% (*v*/v) ACN and 0.1% formic acid, pH 2.9]. The peptides were desalted using reverse phase peptide ChromoLC trap (200 mm × 0.5 mm) column and fractionated in Eksigent C18 column (75 mm × 15 cm) with a flow rate of 300 nL per min using a linear gradient of 2–35% mobile phase B for 99 min (mobile phase A was 0.1% formic acid, and mobile phase B was 100% acetonitrile and 0.1% formic acid). The fractions were analyzed on a TripleTOF 5600 (AB Sciex) mass spectrometer coupled to an Eksigent NanoLC-Ultra 2D plus system. Protein identification and relative quantification were performed by ProteinPilot software (v 4.5; AB Sciex) using the Paragon algorithm with the NCBInr database.

2.9. RNA extraction and quantitative RT-PCR

Total RNA, from the foliar tissues was extracted using lithium chloride method [39]. The concentration of RNA was determined by NanoDrop spectrophotometer. After DNase treatment, the cDNAs were reverse transcribed from 2.0 μg total RNA using c-DNA Synthesis Kit (Thermo Fisher Scientific, USA). The qPCR was performed in ABI PRISM 7700 Real-Time PCR system (Applied Biosystems, USA) using Power SYBR Green PCR Master Mix. The gene-specific cDNA primers were designed by Primer 3 software. Three biological replicates were considered for the analysis and EF1α was used as the internal control.

2.10. Bioinformatics analysis

The graphical and statistical analyses were performed on the data with a one-way analysis of variance (ANOVA) and Duncan's Multiple Range test (DMRT) using GraphPad Prism v 7.00. Gene ontology and KEGG analysis were done using Blast2GO v 4.1.9. In silico localization prediction of the identified proteins and the DRPs were carried out using 5 different prediction tools. These includes WoLF PSORT (http://www.genscript.com/wolf-psort.html), YLoc+ (http://abi.inf.uniuebingen.de/Services/YLoc/webloc.cgi), TargetP (http://www.cbs.dtu.dk/services/TargetP/), MitoFates (http://mitf.cbrc.jp/MitoFates/cgi-bin/top.cgi), Mitoprot (https://ihg.gsf.de/ihg/mitoprot.html). Interactome was developed using StringDB with *Glycine* max as reference interactome map. The identity cutoff for homology was set to 80% and further text processing was done using MySQL and custom PHP scripts. Final interactome was developed using Cytoscape v 3.4.0. For mapping chromosome location, GFF files and sequences were obtained from NCBI *Cicer arietinum* annotation v 101 and used as blast database. Blast parameter was set to evalue of 1e-3 and identity cutoff was fixed at 80%. Maps were created using MapChart Software [40].

3. Results

3.1. Dehydration-induced physiological changes of chickpea seedlings

To understand the dehydration-induced global changes in mitochondrial proteome of chickpea, 3-week-old seedlings were subjected to gradual dehydration by withholding water over 144 h. Previous studies on chickpea established that this period of dehydration treatment is the most representative in view of stress-responsive proteome alterations and other physicochemical indices [41–46]. Initially no morphometric changes were observed in the seedlings. However, the leaflets exhibited rolling and wilting after 48 h of dehydration, and the damage intensified further during 72 h, and this could be observed in about two-third of the stressed seedlings (Fig. 1A). We examined the impact of dehydration on the seedlings by monitoring the photosynthetic efficiency using a LI-6400 system (LI-COR Inc., Nebraska, USA). With progressive dehydration, the rate of photosynthesis and transpiration, stomatal conductance were decreased significantly. The net photosynthetic rate and water transpiration were decreased by 40% after 72 h of dehydration. A decline of the stomatal conductance might be responsible for the decreased photosynthetic rate and water transpiration (Fig. 1B), indicating increased water use efficiency of the seedlings under dehydration. Consequently, under prolonged dehydration the vapour pressure and internal CO_2 concentration were also decreased gradually.

In order to evaluate whether the changes in the physicochemical traits were accompanied by mitochondrial damage, we examined the mitochondrial ultrastructure. The mitochondria were ellipsoid or ovoid with dense matrix and club-shaped cristae. The mitochondrial ultrastructure was significantly altered and more noticeable under severe

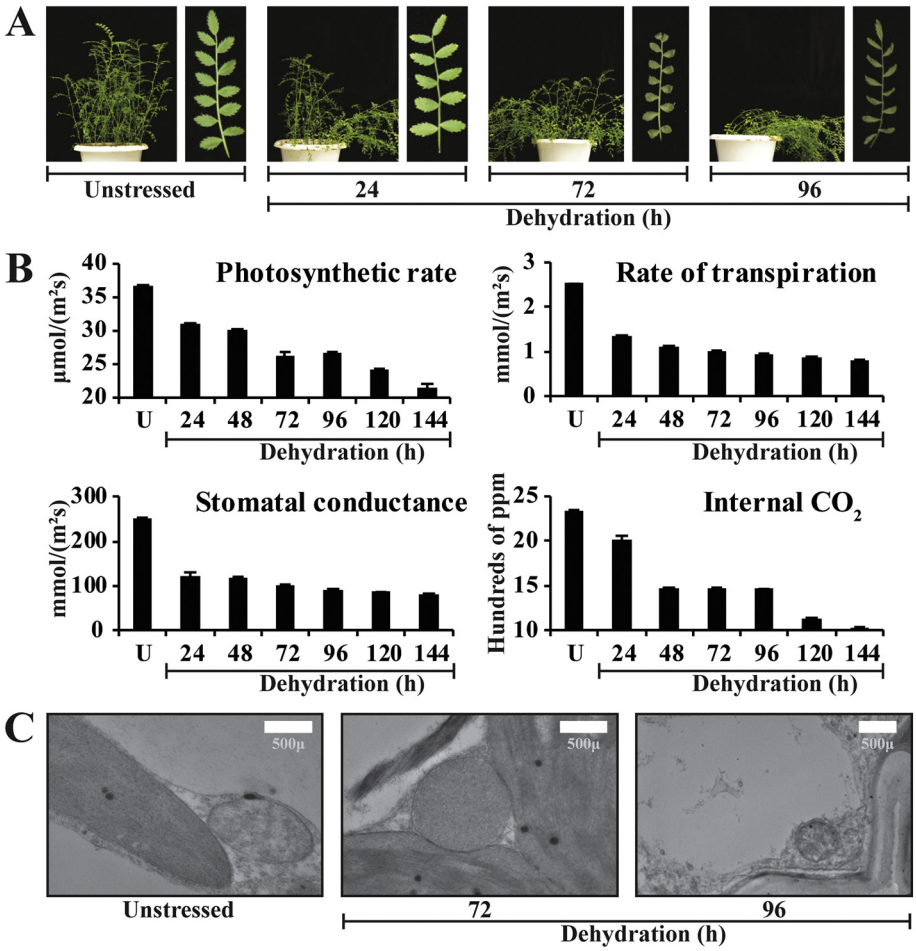

Fig. 1. Morpho-physiological responses of 3-week-old chickpea seedlings under progressive dehydration and changes in mitochondrial ultrastructure. (A) Dehydration-induced morphological changes and leaf senescence under progressive water-deficit stress. (B) Dehydration-induced alterations in photosynthetic rate, transpiration, stomatal conductance and intracellular CO_2 with respect to unstressed seedlings. The experiments were carried out in triplicates (n = 3), and average mean were plotted against treatment time. (C) Micrographs showing the mitochondrial ultrastructure of unstressed control and dehydrated leaves.

dehydration. The mitochondrial damages showed a differential percentage of cristae and volume of electron transparent areas (Fig. 1C). This might be due to the consequence of high sensitivity of mitochondria under water-deficit conditions.

3.2. Isolation of mitochondria and purity assessment

To minimize contamination of other organelles, mitochondrial fraction was isolated by differential centrifugation followed by Percoll density gradient [30,34]. The mitochondria-enriched fraction thus obtained was washed repeatedly to remove the contaminants, if any, from other organelles. Next, the integrity of the mitochondria was examined by staining with Rhodamine-123 fluorescent dye followed by confocal microscopy (Fig. 2A-2C). The micrographs showed intact mitochondria, which were free from other ultrastructural cytoplasmic organelles.

Enrichment of mitochondrial proteins was confirmed by immunological marker, COXII (Fig. 2D). Since chloroplasts are the most likely contaminants associated with the mitochondria, the fraction was tested for most abundant photosynthetic protein Rubisco which displayed negligible presence. The cross contamination of chloroplast was checked using antibodies specific to thylakoid membrane localized LHCII and chloroplast outer envelope membrane translocon complex, TOC75. The immunoblot analysis could not detect chloroplast abundant proteins, LHCII and TOC75 (Fig. 2D). The mitochondrial extracts were further examined for the activity of UGPase, a cytoplasmic enzyme, which was found to be very negligible when compared to the total cell lysate (Fig. 2E). These results together suggest that the mitochondrial fraction was essentially free of chloroplast and cytoplasmic contaminants. In a separate experiment, the integrity of mitochondria was confirmed by the activity of COX, which was markedly increased by the addition of the detergent n-dodecyl- β -D-maltoside (Fig. 2F).

3.3. Global proteomic profiling of mitochondria and identification of dehydration-responsive proteins

To understand the dehydration-induced mitochondrial dynamics, we compared the proteomic profile of treated chickpea seedlings with that of unstressed controls. Two biological replicates were considered for each treatment time-point. The MS/MS spectra were searched against NCBInr database. A total 867 proteins were identified from unstressed tissue, referred to as the mitochondrial proteome reference map (Supplementary Table S1). While there were no detectable contaminants from other organelles, cross contamination cannot absolutely be ruled out due to various technical limitations. In addition, high-sensitivity mass spectrometry might facilitate identification of trace contaminants from other organelles. Therefore, we removed the probable contaminants manually from the list, which yielded 528 proteins (Supplementary Table S2) with molecular mass range 10–100 kDA, and pI range 5–10 (Fig. 3). Localization prediction of the identified proteins (Supplementary Table S3) was accomplished using 5 different prediction algorithm (Mitoprot, YLoc+, TargetP, MitoFates and WoLFPSORT). Notably, each of the programs exercises distinct algorithm for

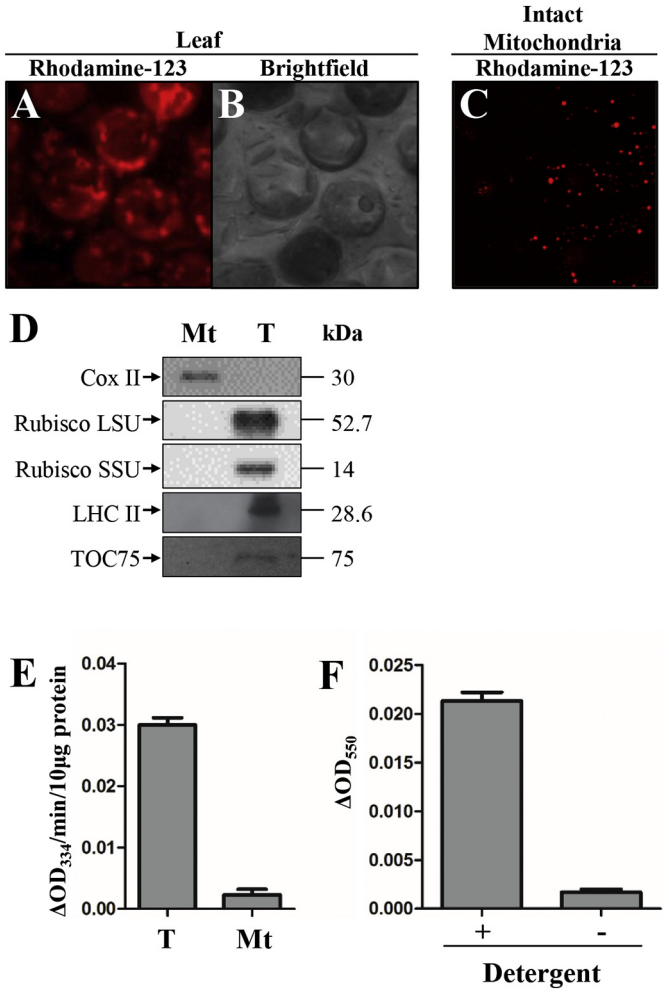

Fig. 2. Purity assessment of mitochondria-enriched fraction. (A) Fluorescence image of Rhodamine-123 stained mitochondria visualized in chickpea leaves, along with the corresponding (B) bright-field image. (C) Rhodamine-123 stained image of mitochondria-enriched fraction. (D) Immunoblot analysis of enriched mitochondrial proteins (Mt) and total cellular proteins (T). The membranes were probed with primary antibodies specific for the target proteins and the signals were detected. (E) Quantitative determination of activities of cytoplasmic marker enzyme, UGPase. (F) Mitochondrial enzyme, cytochrome *c* oxidase (COX) activity measured in presence and absence of detergent.

subcellular prediction and thus produces relatively large non-overlapping sets of results [47]. GO analysis of the reference map showed that major proteins have organic cyclic compound-, heterocyclic compound- and ion-binding function involved in cellular metabolic and organic substance metabolic processes, among others (Supplementary Table S4).

For the identification of DRPs, the cutoff threshold was set to 1% FDR to trade-off quality peptides. The identified protein having unused score ≥ 1.25 were considered as minimum criteria for selection. Those proteins identified in both replicates were considered for further analysis (Supplementary Table S5). The identified 40 DRPs has now been diagrammatically represented according to their degree of upregulation or downregulation (Fig. 3B). The predicted molecular masses of proteins ranged from 10 to 150 kDa, while maximum number of differentially expressed proteins was found to be in the low molecular weight range of 10–50 kDa (Fig. 3C,D). The predicted pI profile of the differentially expressed proteins ranged from pH 4–12 with maximum number of proteins in the range of 5–6 (Fig. 3E,F). Those proteins were considered to be differentially expressed where reporter ion intensity was greater and less than 1.25- and 0.8-fold, respectively when compared with that of unstressed control, and 40 were defined as DRPs (Table 1). The proteins showing consistent up- or down-regulation in both replicates were considered as DRPs. The identified proteins were filtered by population statistic [48–50] to achieve the significantly altered DRPs. The percentage variations among two replicates were plotted against the number of proteins. Only those proteins having < 50% variations were considered for further analysis. The variation between the replicate values of 29 DRPs was < 5%, the remaining showed < 50% variation (Supplementary Fig. S1). Among the DRPs, 24 proteins were upregulated, while 16 were downregulated (Fig. 3A, Table 1).

3.4. Sequence-based localization prediction of the identified DRPs

To predict whether the identified proteins were indeed mitochondrial residents, their amino acid sequences were subjected to multiple prediction programs (Supplementary Table S3). Further, relational evaluation of the overlapping predictions was carried out using different combinations of the programs. The combination of Mitoprot and WoLF PSORT predicted maximum number of proteins to be mitochondrial accounting for 41.1 and 53.98% proteins respectively. Collectively, 352 (66.7%) total and 25 (62.5%) DRPs were predicted to be mitochondrial by at least one program. Altogether, these results showed the limitations in assigning mitochondrial localization based solely on bioinformatics approach. Nevertheless, the choice of prediction softwares can alter different classes of proteins due to the absence of targeting presequences, lack of N-terminal targeting sequences, or due to their incorrect annotation. In addition to the outcome of different prediction softwares, the known and/or predicted localization of the DRPs, are provided in Supplementary Table S3. The localization prediction of the three yet to be characterized proteins in plants, among the identified DRPs, indicated their mitochondrial localization by at least one prediction software. Among them, DUF 3007 superfamily protein was predicted to be mitochondrial by as many as four different softwares. Taken together, the in silico prediction analysis aided in gaining a comprehensive overview of the well-known as well as uncharacterized DRPs.

3.5. Gene ontology based classification of the identified DRPs

The mitochondrial proteome map as well as the DRPs were annotated by BLAST query and classified based on GO term enrichment (Supplementary Table S4, Table 1). The proteins were categorized into different functional ontologies: viz., biological process, cellular compartment and molecular function (Fig. 4A, B). Most of the DRPs were found to be associated with biological processes such as mitochondrial electron transport, ATP synthesis coupled protein transport, biogenesis, stress response and signaling. The major molecular functions associated with the DRPs were oxidation-reduction, transporter and nucleotide binding (Supplementary Table S4). Further, KEGG (Kyoto Encyclopedia of Genes and Genomes) pathway enrichment analysis showed that the differentially expressed proteins were enriched in 33 pathways. The list of DRPs included several enzymes including hydrolases, transferases, oxidoreductase, ligase, isomerase and lyase (Fig. 4C). The functional analysis revealed that majority of dehydration-responsive proteins were involved in purine and thiamine metabolism, carbon fixation pathways and oxidative phosphorylation.

3.6. Chromosomal distribution of the identified DRPs

To investigate the genetic distribution and duplication of the DRPs, we mapped their physical locations on all chromosomes of chickpea. Positions and strand information were derived from GFF file by selective filtering through bash scripts. In case of multiple entries, maximum length open reading frame was taken as a valid connection. Out of 40 differentially expressed genes, 29 were mapped over 8 chromosomes

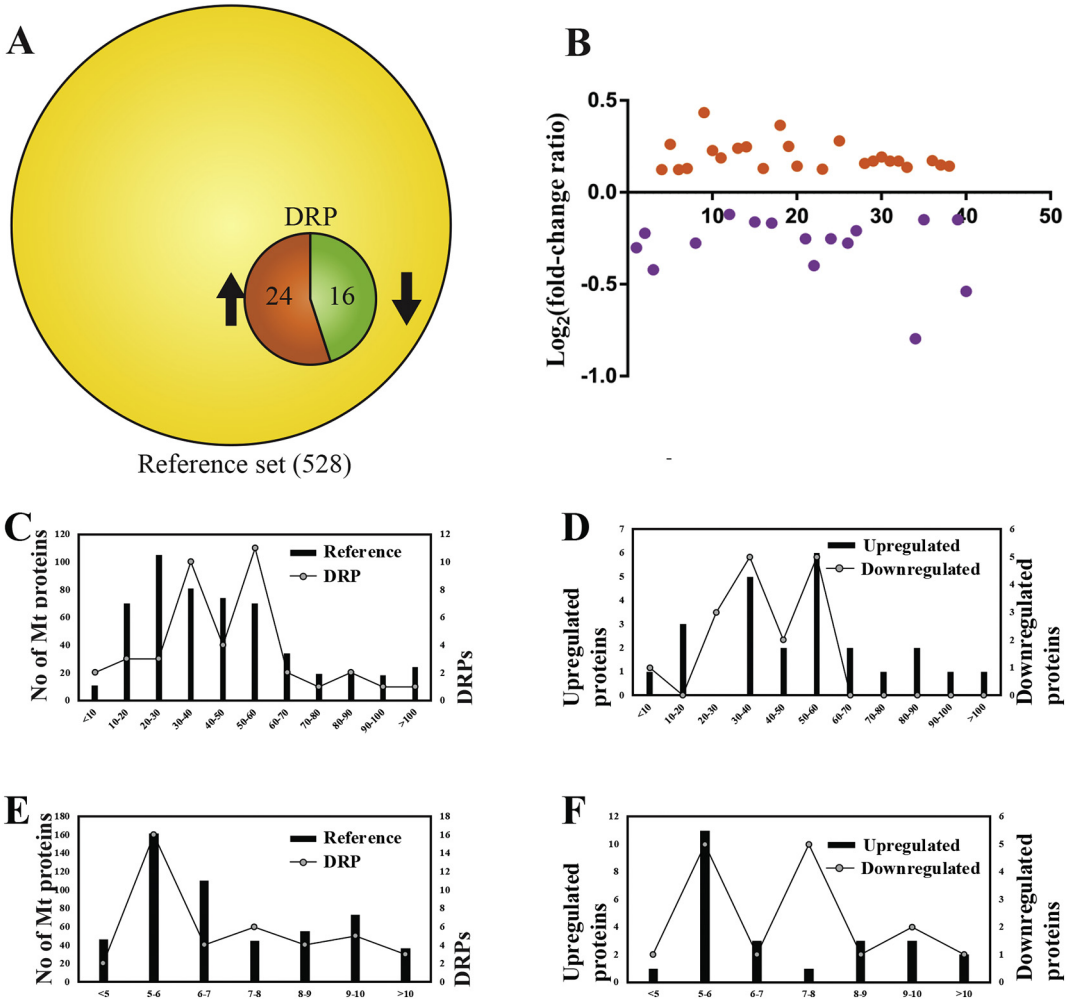

Fig. 3. Characteristics of chickpea mitochondrial proteome. (A). Venn diagram showing number of mitochondria-resident proteins (reference set) as well as dehydration-induced upregulated and downregulated proteins (DRPs). (B) Distribution of log transformed fold change values of the identified DRPs. Histograms represent the distribution of proteins identified in each dataset (reference and DRPs) with respect to the predicted molecular weight (C and D) and isoelectric point (E and F).

(Fig. 5). The genomic sequence of four DRPs viz., BAG family molecular chaperone regulator 7, nucleoside diphosphate kinase 1, protoporphyrinogen oxidase, annexin D1 were not assigned to any particular chromosome, indicating their location in unplaced scaffolds. Since the mitochondrial genome of chickpea is yet to be sequenced, whether the remaining DRPs are encoded in the mitochondrial genome could not be investigated.

3.7. *In silico protein association study of the DRPs*

Protein-protein interaction (PPI) often plays key role in predicting the function of target protein. To gain the mechanistic insight of stress responsive proteins, a protein-protein interaction network was constructed based on predictions, neighborhood analysis, experimental results and literature mining. The PPI network analysis revealed 23 DRPs that play important roles in different cellular functions. The maximum interaction was found among ATPase subunits in the PPI network. Notably, one of the downregulated DRPs, prohibitin, was found to interact with NADH dehydrogenase (Supplementary Fig. S2). The presence of phosphorylation, acetylation or lipid modification were also analyzed (Supplementary Fig. S3 and Supplementary Table S6). Chaperone protein (ClpC) was predicted to interact with two DNAJ10 proteins, both presaged to be acetylated and phosphorylated. Several proteins were predicted to be self-interacting including cytochrome *b* (CytB) and acetyl carboxylase (ACACA). The PPI would facilitate the understanding of underlying molecular mechanisms that might trigger the onset and progression of dehydration.

3.8. *Transcriptional regulation of selected differentially expressed proteins*

Proteomic alterations are often validated by assessment of the transcript abundance of the differentially regulated candidate proteins [51]. To validate the expression of the DRPs, transcript abundance was analyzed by qRT-PCR using gene-specific primers (Supplementary Table S7). In total, eleven genes were randomly selected for expression analysis. Among them, one was upregulated, six were down-regulated and remaining four showed non-significant changes. While both transcript and protein abundance of ATP synthase subunit I was found to be downregulated, reverse pattern of expression was observed in case of ATP synthase subunit β. In case of probable mitochondrial-processing peptidase subunit beta, the transcript and protein abundance showed inverse correlation. Although the transcript abundance was largely consistent with majority of the protein expression data, albeit the fold values of mRNA abundance and protein expression were different (Fig. 6). The differences may be explained in part by technological limitations, and in part by fundamental biological factors in the transcription and translation processes.

Table 1
List of dehydration responsive mitochondrial proteins identified by MS/MS analysis.

Sl. no		Accession	Peptides	% Cov	% Cov (95)	Protein Name	Mean ± SE	Expression
1	Energy metabolism	gi|828,305,948	119	76.3	66.1	PREDICTED: ATP synthase subunit beta [*Cicer arietinum*]	0.71 ± 0.04	DN
2		gi|1,002,266,404	2	12.4	8.8	PREDICTED: NADH dehydrogenase [ubiquinone] flavoprotein 2 [*Oryza sativa* Japonica Group]	0.69 ± 0.06	DN
3		gi|1,003,726,003	42	55.9	39.1	ATPase subunit 1 [*Medicago truncatula*]	0.56 ± 0.07	DN
4		gi|1,026,012,753	21	16.2	10.3	PREDICTED: cytochrome *b*-like [*Capsicum annuum*]	0.62 ± 0.04	DN
5		gi|502,111,827	5	36.1	36.1	PREDICTED: cytochrome *b*-c1 complex subunit 9 [Cicer arietinum]	1.33 ± 0.05	UP
6	Biogenesis	gi|502,127,259	17	62.6	50	PREDICTED: prohibitin-3 [Cicer arietinum]	0.50 ± 0.00	DN
7	Stress response	gi|502,173,457	2	26.2	12.1	PREDICTED: nucleoside diphosphate kinase 1 [Cicer arietinum]	1.78 ± 0.26	UP
8		gi|950,971,152	2	8.6	8.6	PREDICTED: annexin-like protein RJ4 [*Vigna radiata* var. *radiata*]	1.77 ± 0.51	UP
9		gi|502,169,040	3	17.3	8.7	PREDICTED: BAG family molecular chaperone regulator 7 [Cicer arietinum]	1.39 ± 0.08	UP
10		gi|502,178,095	3	8.5	8.5	PREDICTED: annexin D1 [Cicer arietinum]	1.44 ± 0.03	UP
11		gi|645,262,825	2	10	8.6	PREDICTED: chaperone protein dnaJ 10 [*Prunus mume*]	0.53 ± 0.03	DN
12		gi|590,691,084	2	4.6	3.7	26S proteasome regulatory subunit S2 1A isoform 8 [*Theobroma cacao*]	1.41 ± 0.03	UP
13		gi|502,167,290	2	14.1	5.3	PREDICTED: 3-deoxy-manno-octulosonate cytidylyltransferase [Cicer arietinum]	0.68 ± 0.03	DN
14		gi|502,118,050	1	10.4	5.4	PREDICTED: probable glutathione S-transferase isoform X1 [Cicer arietinum]	0.60 ± 0.17	DN
15		gi|502,158,766	1	16.8	3.4	PREDICTED: chaperone protein dnaJ 10 [Cicer arietinum]	0.29 ± 0.12	DN
16	Signaling	gi|525,314,407	14	68.3	46.2	plasma membrane-associated cation-binding protein 1-like [Cicer arietinum]	0.76 ± 0.04	DN
17		gi|502,139,691	2	7.8	7.8	PREDICTED: calcium-dependent protein kinase SK5 [Cicer arietinum]	2.32 ± 0.96	UP
18	Metabolism	gi|828,309,883	8	22.9	18.2	PREDICTED: serine–glyoxylate aminotransferase isoform X2 [Cicer arietinum]	1.48 ± 0.12	UP
19		gi|502,077,377	3	4.3	4.3	PREDICTED: fatty acid amide hydrolase isoform X1 [Cicer arietinum]	1.35 ± 0.09	UP
20		gi|242,065,996	6	9	9	hypothetical protein SORBIDRAFT_04g028050 [*Sorghum bicolor*]	0.40 ± 0.23	DN
21		gi|502,130,304	3	4	2.3	PREDICTED: acetyl-CoA carboxylase 1-like [Cicer arietinum]	1.91 ± 0.02	UP
22		gi|828,324,680	6	11.9	8.1	PREDICTED: xylose isomerase [Cicer arietinum]	0.38 ± 0.12	DN
23		gi|502,148,189	4	15.7	9.2	PREDICTED: ACT domain-containing protein ACR11-like [Cicer arietinum]	1.33 ± 0.05	UP
24		gi|502,174,085	1	9.6	2.4	PREDICTED: protoporphyrinogen oxidase [Cicer arietinum]	1.48 ± 0.17	UP
25		gi|502,129,455	3	17.6	14.7	PREDICTED: cinnamoyl-CoA reductase 1 [Cicer arietinum]	1.34 ± 0.07	UP
26		gi|502,116,230	2	7.7	6	PREDICTED: ureidoglycolate hydrolase [Cicer arietinum]	1.69 ± 0.43	UP
27	Transport activity	gi|694,361,837	6	13.2	10.2	PREDICTED: probable mitochondrial-processing peptidase subunit beta isoform X1 [Pyrus x bretschneideri]	1.48 ± 0.13	UP
28		gi|703,107,464	2	6.6	4	ADP-ribosylation factor 1 [Morus notabilis]	1.83 ± 0.53	UP
29		gi|502,083,669	4	7.3	5.6	PREDICTED: protein TIC 100 [Cicer arietinum]	1.74 ± 0.42	UP
30		gi|502,077,851	5	12.9	10.1	PREDICTED: clathrin light chain 1-like [Cicer arietinum]	1.35 ± 0.00	UP
31		gi|502,145,464	9	13.4	10.7	PREDICTED: alpha carbonic anhydrase 7-like [Cicer arietinum]	0.71 ± 0.05	DN
32		gi|502,152,309	3	10	7.7	PREDICTED: peroxisomal membrane protein PEX14 [Cicer arietinum]	2.72 ± 1.26	UP
33		gi|922,362,028	2	4.7	1.8	Exocyst complex component 84B [Medicago truncatula]	1.49 ± 0.22	UP
34	RNA binding	gi|955,324,391	1	4.6	2.6	PREDICTED: RNA-binding protein 39 isoform X2 [*Glycine max*]	1.56 ± 0.17	UP
35	DNA binding	gi|848,862,394	18	40.4	39.1	PREDICTED: histone H2A-like [Erythranthe guttata]	1.39 ± 0.12	UP
36		gi|743,941,248	8	50	45.5	PREDICTED: probable histone H2A variant 3 [Populus euphratica]	1.37 ± 0.09	UP
37	Protein synthesis	gi|828,332,117	1	5.5	2	PREDICTED: eukaryotic peptide chain release factor GTP-binding subunit-like isoform X2 [Cicer arietinum]	0.53 ± 0.27	DN
38	Uncharacterized protein	gi|702,271,685	3	18.2	18.2	PREDICTED: uncharacterized protein LOC104432752 [*Eucalyptus grandis*]	0.56 ± 0.02	DN
39		gi|502,138,028	3	11.8	11.8	PREDICTED: uncharacterized protein LOC101492666 [Cicer arietinum]	0.16 ± 0.01	DN
40		gi|593,782,269	2	2.6	2.6	hypothetical protein PHAVU_003G096500g [*Phaseolus vulgaris*]	1.54 ± 0.12	UP

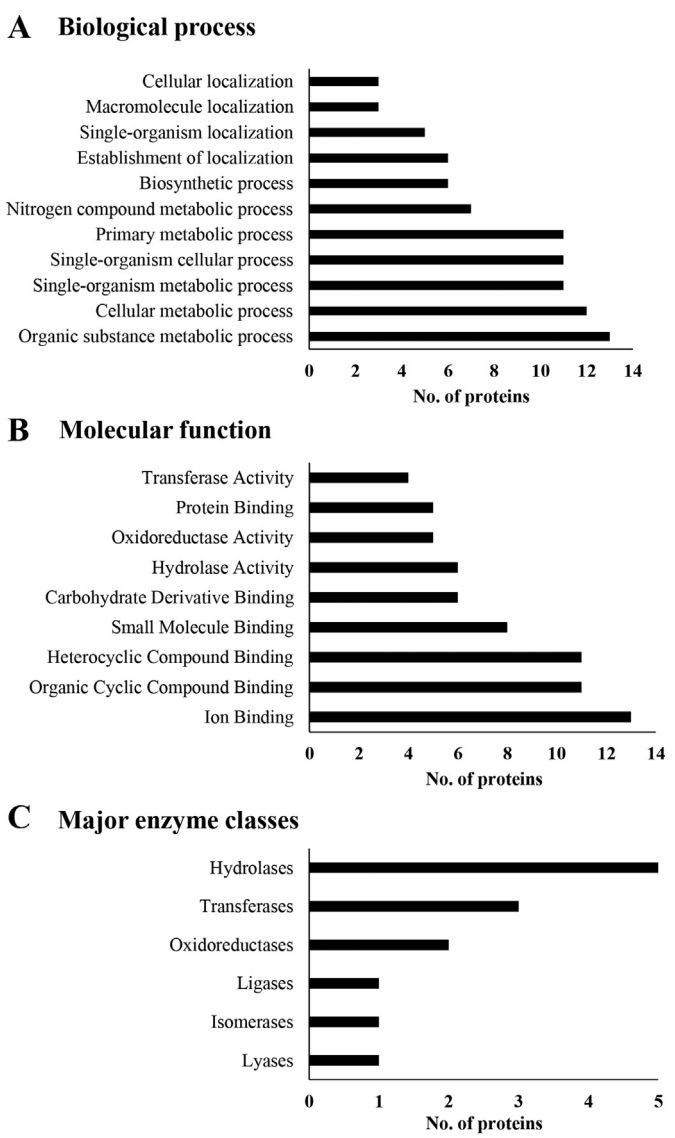

Fig. 4. Gene ontology classification of differentially expressed mitochondrial proteins by sequence similarity search against NCBI database. Bar diagrams displaying distribution of proteins according to their involvement in different (A) biological processes and (B) molecular functions. (C) KEGG analysis showing major enzyme classes.

3.9. Dehydration-induced alteration of mitochondrial ATP production and respiratory O_2 consumption

Mitochondria generates most of the ATP by using proton motive force generated via electron transport chain (ETC) during electron transfer from reducing equivalents to oxygen. We therefore sought to know how dehydration-induced changes in the proteome network impact mitochondrial ATP production and respiratory O2 consumption. The effect of dehydration stress on mitochondrial function was assessed by estimation of ATP content and respiratory O_2 consumption in the mitochondria isolated from unstressed control and 72-h dehydrated seedlings. The luciferase based assay demonstrated that ATP content of mitochondria decreased significantly post-dehydration as compared to unstressed control (Fig. 7A). Subsequently, mitochondrial O_2 consumption was also found to be significantly decreased under dehydration (Fig. 7B). Integration of stress-responsive proteome alterations with functional data suggest a potential link between the molecular basis of stress response and mitochondrial energy transduction.

3.10. Identification of dehydration-responsive mitochondrial protein, CaPHB1

A critical screening of the mitochondrial proteome led to the identification of a prohibitin, henceforth designated CaPHB1, which exhibited markedly downregulated expression. Prohibitin is a member of a superfamily of ubiquitously expressed and evolutionarily conserved proteins [52,53]. Plant prohibitins are localized largely in the mitochondria and involved in mitochondrial biogenesis [54–56]. Notably while CaPHB1 is known to be involved in mitochondrial biogenesis, its role in stress tolerance is yet to be established. CaPHB1 (GI:502127259) comprises 278 amino acids, which would encode a protein with an estimated molecular mass of 30 kDa. The chickpea prohibitin, *CaPHB1*, is located on chromosome 5 (9075150–9,079,327 complement strands). The coding sequence for *CaPHB1* is 837 bp, which extends over a span of 4178 bp on the chickpea genome and is interrupted by 2 introns. The first and second exons code for both coding region and UTR, while exon-3 consists of UTR only (Fig. 8A).

Phylogenetic analysis of 11 chickpea prohibitins along with 7 Arabidopsis homologs indicated that *CaPHB1* belong to prohibitin-1 family along with XP_004511131, AtPHB3, AtPHB4 and AtPHB7 as reported earlier [30]. AtPHB1, AtPHB2, AtPHB5 and AtPHB6 have been reported as members of prohibitin-2 family. The remaining 9 proteins belong to prohibitin-2 family, albeit they appear to belong to two separate lineages (Fig. 8B). Domain analysis showed that all chickpea prohibitins contain a single stretch of band_7 domain characterized as prohibitin family except XP_0045027083.1, which contains an additional stretch of band_7_c and is identical to bacterial prohibitin.

To gain insight into the probable functional properties of CaPHB1, the 3D structure was generated (Fig. 8C) using intensive mode in Phyre 2 server [57]. The secondary structure showed the presence of 8 alpha helices and 4 beta sheets, and 32 residues predicted to have disorder, imparting CaPHB1 the ability to protect plants against stress and senescence. Promoter analysis through PlantCARE database showed that CaPHB1 might be controlled by gibberellins (Fig. 8D).

The transcriptional regulation of CaPHB1 under dehydration revealed a significant increase in expression (Fig. 9). Dehydration-responsive pathway often overlaps with that of oxidative stress [58–60], and thus the expression of *CaPHB1* in chickpea was investigated under MV-induced oxidative stress. There was a significant decline in *CaPHB1* transcripts by MV when compared with the unstressed condition (Fig. 9). Ethylene-JA signaling pathways have previously been demonstrated to be a major part of plant defense reactions against pathostress [61–63]. The *CaPHB1* transcripts were highly induced by exogenous ethylene treatment, but markedly decreased by JA (Fig. 9). Next, we examined whether *CaPHB1* transcription was affected by ABA, which showed enhanced ABA sensitivity. These results altogether suggest that *CaPHB1* may actively participate in both biotic and abiotic stresses, possibly through antagonistic interactions between ABA and the JA-ethylene signaling pathways.

4. Discussion

Mitochondria, being the primary energy-generating system in most eukaryotic cells, contribute to various metabolic processes [47], and respond rapidly to stress. The stress-induced alterations are accomplished by multi-component molecular machineries, which consists of several stress-responsive proteins. Therefore, to identify the key proteomic components whose levels alter under dehydration, we investigated the reference and dehydration-responsive mitochondrial proteome of chickpea. A relatively dehydration tolerant ecotype, variety JG-62 [64,65], was used to understand the machinery required for stress-adaptation. The severity of dehydration stress was assessed by analyzing morphological and physicochemical alterations of the stressed seedlings (Fig. 1). The observed decrease in photosynthetic efficiency might be a consequence of declined osmotic potential under

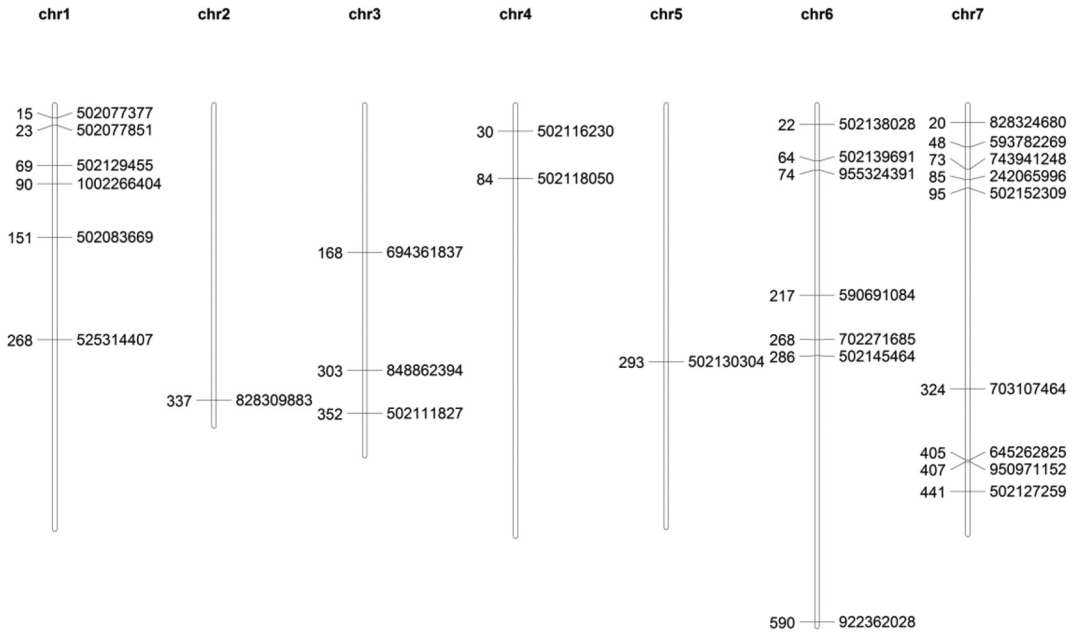

Fig. 5. Chromosomal distribution of the differentially expressed mitochondrial proteins represented by corresponding accession numbers. (For interpretation of the references to colour in this figure legend, the reader is referred to the web version of this article.)

dehydration [66], which corroborates the earlier reports [65,66] of plant response to water-deficit conditions. The changes in morphological and physicochemical properties were accompanied by damage in mitochondrial ultrastructure under water-deficit conditions.

Next, to correlate the decline in physiological functions with proteomic alterations, dehydration-induced global changes of the mitochondrial proteome was quantified, which led to the identification of 40 DRPs. Functional classification of the DRPs revealed their involvement in energy metabolism, stress response, signaling and transport (Table 1). Of the DRPs involved in energy metabolism, ATP synthase,

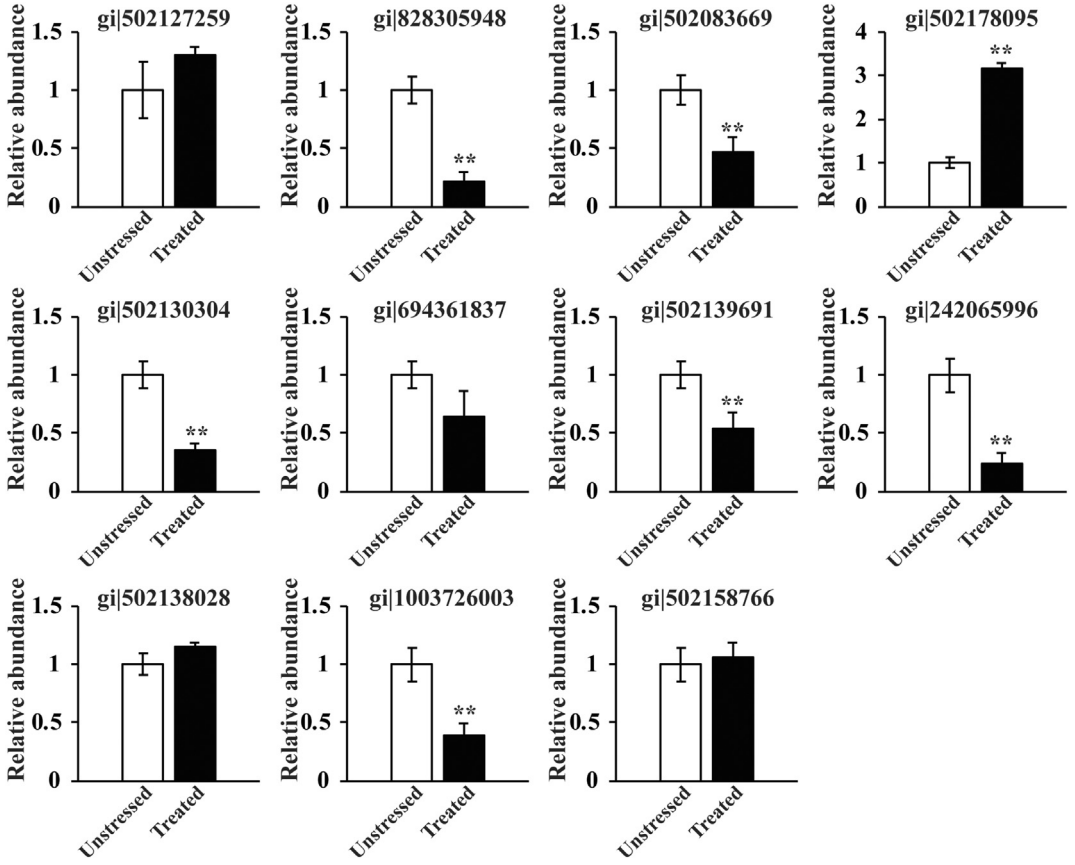

Fig. 6. Relative mRNA abundance of 11 randomly selected DRPs. cDNA was prepared using mRNA from unstressed control and 72-h dehydrated tissues. The values are represented as the means from three independent triplicates. Asterisk indicates a significant difference from the unstressed control ($*p < .05$).

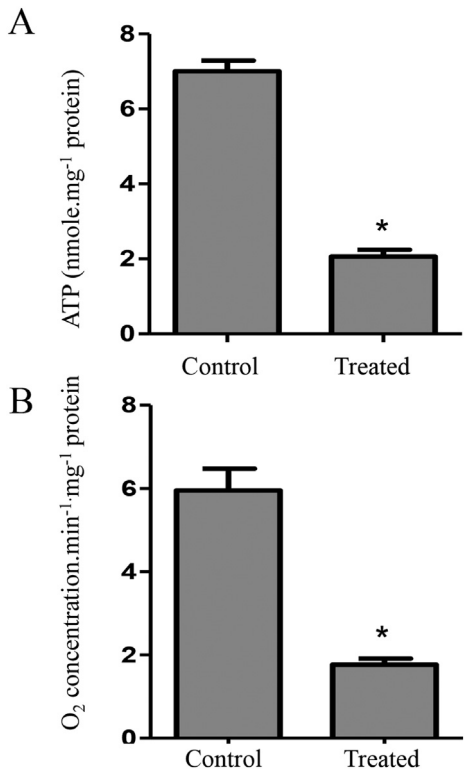

Fig. 7. Changes in mitochondrial metabolic function. The ATP abundance (A) and O_2 consumption (% in air saturation) (B) were determined in the mitochondria isolated form unstressed control and dehydration treated seedlings. The measurements were done in triplicates. Asterisk indicate significant difference from unstressed control (*$p < .05$).

subunits showed downregulation, which explains the observed decrease in ATP abundance in the mitochondria isolated from stressed seedlings. Also, ATP synthase is reported to play a central role in mitochondrial permeability transition (MPT), wherein a rapid increase in the inner mitochondrial membrane permeability to low molecular weight solutes takes place [67]. The dehydration-induced downregulation of ATP synthase β-subunit might alter the permeability of the inner mitochondrial membrane and the resultant osmotic influx of water into the mitochondria might have resulted in structural and functional collapse. Nucleoside diphosphate kinase 1 (NDK1) is responsible for exchange of phosphate between a nucleoside triphosphate (NTP) and a nucleoside diphosphate (NDP) and its increased expression has earlier been reported in pea, under heat stress [68]. Annexins are known to play crucial role in abiotic stress responses by regulation of H_2O_2 homeostasis [69]. Stress-induced increase in mitochondrial annexin-like protein RJ4 indicates cellular efforts toward the maintenance of ROS homeostasis. The expression of a BAG family protein was highly induced in this study, indicating its significant involvement in dehydration response. The BAG proteins are a family of chaperones, which interacts with Hsp70 and are earlier reported to confer tolerance to pathogen attack and abiotic stress [70]. Another dehydration-responsive element was 26S proteasome regulatory subunit, which displayed increased expression, presumably as a damage control attempt [71]. Another downregulated DRP, DnaJ proteins function as molecular chaperone and play important role in plant growth and development in response to abiotic stress [72]. The identification of overlapping proteins in response to dehydration as well as other stresses indicate cross-talk among different stress-responsive pathways.

Among the DRPs involved in metabolism, serine glyoxylate aminotransferase that predominantly catalyzes glycine biosynthesis was highly upregulated, and was consistent with its dehydration-induced expression in *M. domestica* [73]. Fatty acid amide hydrolases (FAAH) are serine hydrolases, which plays key role in plant innate immunity [74]. The increased abundance of FAAH observed, in this study, indicates its role in abiotic stress. Xylose isomerase, involved in cellulose biosynthesis, showed dehydration-induced downregulation, which is consistent with earlier reports in Arabidopsis, and wheat [75]. Protoporphyrinogen oxidase (PPO), an enzyme found both in chloroplast and mitochondria, showed considerable upregulation. Overexpression of PPO has previously been shown to enhance stress tolerance in rice [76]. Further, the upregulation of DNA-binding histone H2A-like protein indicates dehydration-induced shift in chromatin regulation. The stress-induced upregulation of mitochondrial processing peptidase transporter and CDPK-SK5 is consistent with earlier reports [43,77]. The list of DRPs also included proteins such as PEX14, which is reported to be chloroplast residents. However, PEX14 has previously been shown to be imported to mitochondria in mammalian system [78]. Therefore, multiple subcellular localization of such proteins in plants cannot be ruled out, albeit this needs further experimental validation.

Several DRPs, identified in this study, have so far not been reported to be mitochondrial residents. For instance, alpha carbonic anhydrase (αCA) 7-like, a downregulated DRP, although predicted to be chloroplast-resident in Arabidopsis [79], there has been no report on its subcellular localization. We report, for the first time, the proteomic identification of αCA and its dehydration-induced alterations. Another upregulated DRP, BAG family molecular chaperone regulator 7, belongs to BAG family of proteins which are known to localize in nucleus or cytoplasm in the mammals. However, such proteins are reported to have more diverse localizations in plants, including mitochondria and vacuoles [80]. Yet another highly upregulated DRP, PEX 14, is reported to be one of the integral peroxisomal membrane proteins that are imported to the mitochondria [78]. Further, in silico analysis by Mitoprot predicted mitochondrial localization of calcium dependent protein kinase (CDPK), SK5. The CDPKs are reported be distributed in multiple subcellular compartments viz., PM, nucleus, cytosol, ER and peroxisomes, besides mitochondria. DRPs such as DNAJ 10 chaperone, involved in plant development [81], was predicted to be mitochondria-resident by WoLF PSORT. Intriguingly, none of the histone variants, identified in this study, were predicted to be mitochondrial residents. However, mitochondrial histones and their multiple roles are well established [82]. While proteins such as annexin-like protein RJ4 and DI have so far not been reported from chickpea, mitochondrial association of annexins have long been established [83]. Notably, multi-locational distribution of proteins is increasingly evident, particularly by the interaction between the energy organelles and their functional coordination in execution and regulation of metabolic functions [84,85].

Among the identified DRPs involved in key biological processes was prohibitin 1, known to be involved in mitochondrial biogenesis [86], but its role in stress tolerance is yet to be established. The expression of chickpea prohibitin 1, CaPHB1, was markedly reduced with increasing dehydration. The transcript analysis showed that *CaPHB1* might participate in multivariate stress adaptation, possibly via ABA-independent pathways. Furthermore, PPI network analysis revealed interaction between CaPHB1 and NADH dehydrogenase.

One of the detrimental effects of water-deficit conditions is exerted by affecting mitochondrial respiration, the levels of which maintains carbon balance and plant productivity. Maintenance of mitochondrial respiration is critical for plant growth and survival under both well-watered and water-deficit conditions. Dehydration-induced alterations in mitochondrial proteome identified NADH dehydrogenase as one of the downregulated DRPs. NADH dehydrogenase functions in the conversion of NADH into NAD and H+ in mitochondrial complex I. The released H+ ion is important for the regulation of proton electrochemical gradient and reduction of O_2 into water. Determination of O_2 consumption showed a sharp decline in the mitochondria isolated from stressed seedlings when compared with that in unstressed control. The proteome level alteration of NADH dehydrogenase directly corroborated with the decline in mitochondrial respiration. Additionally, ATP

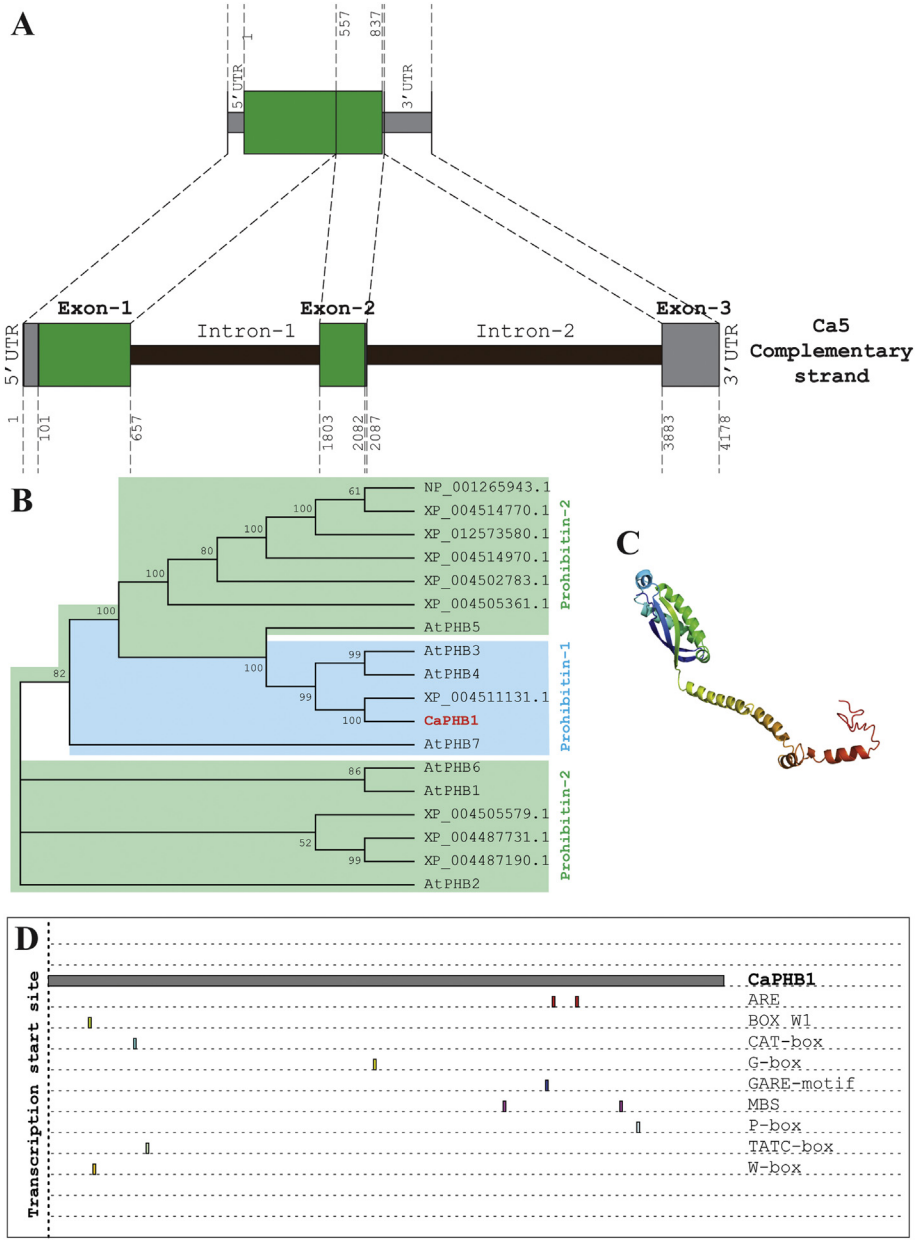

Fig. 8. Structural organization and phylogenetic analysis of *CaPHB1*. (A) Schematic illustration of the genomic organization of *CaPHB1*. (B) Phylogram, constructed by neighbour-joining method, showing the relationship of *CaPHB1* (marked in red) with other prohibitins of chickpea and Arabidopsis. (C) 3D structure of CaPHB1 predicted by Phyre2. (D) Representation of significant regulatory elements in upstream promoter sequence of *CaPHB1* as predicted by PlantCARE. (For interpretation of the references to colour in this figure legend, the reader is referred to the web version of this article.)

synthase subunit beta showed dehydration-induced. Together, these results provide new insights into dehydration-induced mitochondrial dysfunction, which might help understand the adaptive process.

5. Conclusion

In this study, we investigated the effect of dehydration on mitochondrial proteome landscape of chickpea, the most cultivated legumes in the world. This is the first report of mitochondrial proteome alteration in a legume caused by water-deficit stress. We aimed at comparing dehydration-induced mitochondrial protein expression and identifying differentially expressed proteins. The proteomics analysis led to the identification of dehydration-responsive 40 mitochondrial proteins, regulating diverse biological processes and cellular functions. The expression of DRPs was positively correlated with dehydration-induced mRNA abundance. Screening of the proteome suggests that CaPHB1 is a potential mitochondrial protein that has a critical function in mitochondrial biogenesis, and may play a role in regulating defense response. While the precise molecular mechanism of how CaPHB1 function remains to be investigated, this is clear that CaPHB1 participates in multivariate stress responses in chickpea. Protein association mapping revealed interaction between CaPHB1 with NADH dehydrogenase, which was also found to be downregulated under dehydration. This downregulation corroborated with the decline in mitochondrial O_2 consumption and ATP synthesis.

Supplementary data to this article can be found online at https://doi.org/10.1016/j.jprot.2018.09.008.

Declaration

The authors declare no conflict of interest.

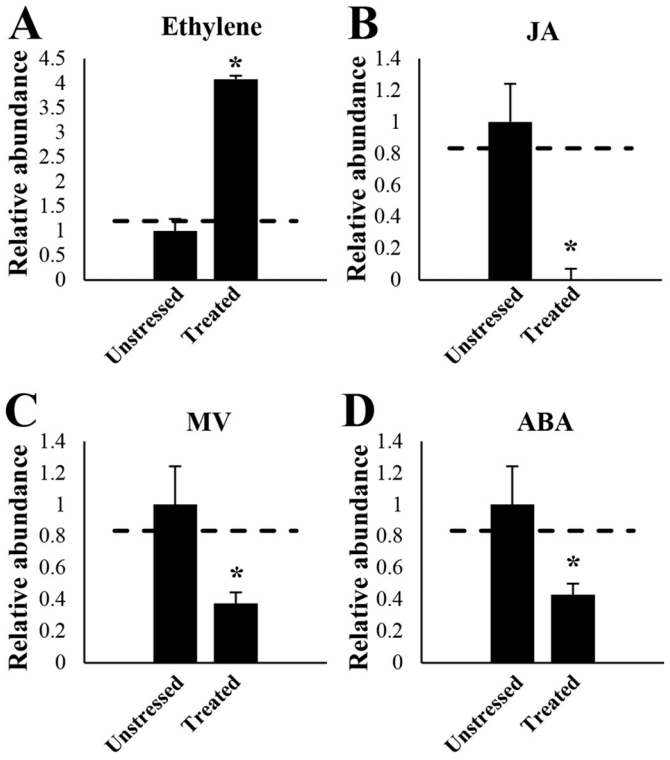

Fig. 9. qRT-PCR analysis showing differential accumulation of *CaPHB1* transcript in response to various treatments viz., (A) ethylene (0.5 μM), (B) JA (100 μM), (C) MV (100 μM) and (D) ABA (100 μM). The expression levels of *CaPHB1* were normalized with the internal control *EF1α*. Error bars represent the SE from three independent replicates. Asterisk shows significant differences with respect to unstressed control ($*p < .05$).

Acknowledgements

This work was supported by grants from the Department of Biotechnology (DBT), India (BT/AGR/CG-PhaseII/01/2014) and National Institute of Plant Genome Research, New Delhi to N.C. We thank Department of Science and Technology (DST), India for SERB-National Post-Doctoral Fellowship (PDF/2016/002615) granted to D.G. and Council of Scientific & Industrial Research (CSIR), India for providing pre-doctoral fellowship to S.G. and N.V.L. We also acknowledge DBT for providing pre-doctoral fellowship to P.B. We thank Dr. J.G Kapuganti and Dr. Sonika Pandey for valuable suggestions and guidance in measurement of mitochondrial respiration parameters. We thank Mr. Jasbeer Singh for illustrations and graphical representation in the manuscript.

References

[1] L. Cattivelli, F. Rizza, F.-W. Badeck, E. Mazzucotelli, A.M. Mastrangelo, E. Francia, C. Mare, A. Tondelli, A.M. Stanca, Drought tolerance improvement in crop plants: an integrated view from breeding to genomics, Field Crops Res. 105 (2008) 1–14.
[2] J. Kashiwagi, L. Krishnamurthy, P. Gaur, H. Upadhyaya, R. Varshney, S. Tobita, Traits of relevance to improve yield under terminal drought stress in chickpea (*C. arietinum* L.), Field Crops Res. 145 (2013) 88–95.
[3] Y. Osakabe, K. Osakabe, K. Shinozaki, L.-S.P. Tran, Response of plants to water stress, Front. Plant Sci. 5 (2014) 86.
[4] H. Lafitte, G. Yongsheng, S. Yan, Z. Li, Whole plant responses, key processes, and adaptation to drought stress: the case of rice, J. Exp. Bot. 58 (2006) 169–175.
[5] M. Nakajima, A. Enju, T. Sakurai, M. Satou, K. Akiyama, T. Taji, K. Yamaguchi-Shinozaki, P. Carninci, J. Kawai, Y. Hayashizaki, Monitoring the expression proles of 7000 Arabidopsis genes under drought, cold and high-salinity stresses using a full-length cDNA microarray, Plant J. 31 (2002) 279–292.
[6] D.W. Hopper, R. Ghan, K.A. Schlauch, G.R. Cramer, Transcriptomic network analyses of leaf dehydration responses identify highly connected ABA and ethylene signaling hubs in three grapevine species differing in drought tolerance, BMC Plant Biol. 16 (2016) 118.
[7] G.K. Agrawal, J. Bourguignon, N. Rolland, G. Ephritikhine, M. Ferro, M. Jaquinod, K.G. Alexiou, T. Chardot, N. Chakraborty, P. Jolivet, Plant organelle proteomics: collaborating for optimal cell function, Mass Spc. Rev. 30 (2011) 772–853.
[8] J. Hu, C. Rampitsch, N.V. Bykova, Advances in plant proteomics toward improvement of crop productivity and stress resistance, Front. Plant Sci. 6 (2015) 209.
[9] R.P. Jacoby, L. Li, S. Huang, C. Pong Lee, A.H. Millar, N.L. Taylor, Mitochondrial composition, function and stress response in plants, J.Int. Plant Biol. 54 (2012) 887–906.
[10] J.F. Havelund, J.J. Thelen, I.M. Møller, Biochemistry, proteomics, and phosphoproteomics of plant mitochondria from non-photosynthetic cells, Front. Plant Sci. 4 (2013).
[11] K.L. Liberatore, S. Dukowic-Schulze, M.E. Miller, C. Chen, S.F. Kianian, The role of mitochondria in plant development and stress tolerance, Free Radic. Biol. Med. 100 (2016) 238–256.
[12] C.B. Epstein, J.A. Waddle, W. Hale, V. Davé, J. Thornton, T.L. Macatee, H.R. Garner, R.A. Butow, Genome-wide responses to mitochondrial dysfunction, Mol. Biol. Cell 12 (2001) 297–308.
[13] O.K. Atkin, D. Macherel, The crucial role of plant mitochondria in orchestrating drought tolerance, Ann. Bot. 103 (2008) 581–597.
[14] R. Rao, F. Salvato, B. Thal, H. Eubel, J. Thelen, I. Møller, The proteome of higher plant mitochondria, Mitochondrion 33 (2017) 22–37.
[15] X. Pu, X. Lv, T. Tan, F. Fu, G. Qin, H. Lin, Roles of mitochondrial energy dissipation systems in plant development and acclimation to stress, Ann. Bot. 116 (2015) 583–600.
[16] N.L. Taylor, J.L. Heazlewood, D.A. Day, A.H. Millar, Differential impact of environmental stresses on the pea mitochondrial proteome, Mol. Cell. Proteomics 4 (2005) 1122–1133.
[17] W.Q. Wang, H.Y. Cheng, I.M. Møller, S.Q. Song, The role of recovery of mitochondrial structure and function in desiccation tolerance of pea seeds, Physiol. Plant. 144 (2012) 20–34.
[18] J. Grelet, A. Benamar, E. Teyssier, M.-H. Avelange-Macherel, D. Grunwald, D. Macherel, Identification in pea seed mitochondria of a late-embryogenesis abundant protein able to protect enzymes from drying, Plant Physiol. 137 (2005) 157–167.
[19] D. Macherel, A. Benamar, M.H. Avelange-Macherel, D. Tolleter, Function and stress tolerance of seed mitochondria, Physiol. Plant. 129 (2007) 233–241.
[20] D. Tolleter, D.K. Hincha, D. Macherel, A mitochondrial late embryogenesis abundant protein stabilizes model membranes in the dry state, Biochim. Biophys. Acta Biomembr. 1798 (2010) 1926–1933.
[21] M.H. Avelange-Macherel, N. Payet, D. Lalanne, M. Neveu, D. Tolleter, J. Burstin, D. Macherel, Variability within a pea core collection of LEAM and HSP22, two mitochondrial seed proteins involved in stress tolerance, Plant Cell Env. 38 (2015) 1299–1311.
[22] D. Tolleter, M. Jaquinod, C. Mangavel, C. Passirani, P. Saulnier, S. Manon, E. Teyssier, N. Payet, M.-H. Avelange-Macherel, D. Macherel, Structure and function of a mitochondrial late embryogenesis abundant protein are revealed by desiccation, Plant Cell 19 (2007) 1580–1589.
[23] A. Candat, G. Paszkiewicz, M. Neveu, R. Gautier, D.C. Logan, M.-H. Avelange-Macherel, D. Macherel, The ubiquitous distribution of late embryogenesis abundant proteins across cell compartments in Arabidopsis offers tailored protection against abiotic stress, Plant Cell 26 (2014) 3148–3166.
[24] E. Jaspard, D. Macherel, G. Hunault, Computational and statistical analyses of amino acid usage and physico-chemical properties of the twelve late embryogenesis abundant protein classes, PLoS One 7 (2012) e36968.
[25] W.Q. Wang, Y. Wang, Q. Zhang, I.M. Møller, S.Q. Song, Changes in the mitochondrial proteome of developing maize seed embryos, Physiol. Plant. 163 (2018) 552–572.
[26] G. Yin, H. Sun, X. Xin, G. Qin, Z. Liang, X. Jing, Mitochondrial damage in the soybean seed axis during imbibition at chilling temperatures, Plant Cell Physiol. 50 (2009) 1305–1318.
[27] S. Komatsu, D. Thibaut, S. Hiraga, M. Kato, M. Chiba, A. Hashiguchi, M. Tougou, S. Shimamura, H. Yasue, Characterization of a novel flooding stress-responsive alcohol dehydrogenase expressed in soybean roots, Plant Mol. Biol. 77 (2011) 309–322.
[28] A.H.M. Kamal, S. Komatsu, Involvement of reactive oxygen species and mitochondrial proteins in biophoton emission in roots of soybean plants under flooding stress, J. Proteome Res. 14 (2015) 2219–2236.
[29] M. Rurek, A.M. Woyda-Ploszczyca, W. Jarmuszkiewicz, Biogenesis of mitochondria in cauliflower (Brassica oleracea var. botrytis) curds subjected to temperature stress and recovery involves regulation of the complexome, respiratory chain activity, organellar translation and ultrastructure, Biochim. Biophys. Acta Bioenerg. 1847 (2015) 399–417.
[30] F. Salvato, J.F. Havelund, M. Chen, R.S.P. Rao, A. Rogowska-Wrzesinska, O.N. Jensen, D.R. Gang, J.J. Thelen, I.M. Møller, The potato tuber mitochondrial proteome, Plant Physiol. 164 (2013) 637–653.
[31] J. Senkler, M. Senkler, H. Eubel, T. Hildebrandt, C. Lengwenus, P. Schertl, M. Schwarzländer, S. Wagner, I. Wittig, H.P. Braun, The mitochondrial complexome of Arabidopsis thaliana, Plant J. 89 (2017) 1079–1092.
[32] N.A. Karp, K.S. Lilley, Investigating sample pooling strategies for DIGE experiments to address biological variability, Proteomics 9 (2009) 388–397.
[33] D. Sosso, S. Mbelo, V. Vernoud, G. Gendrot, A. Dedieu, P. Chambrier, M. Dauzat, L. Heurtevin, V. Guyon, M. Takenaka, PPR2263, a DYW-subgroup pentatricopeptide repeat protein, is required for mitochondrial nad5 and cob transcript editing, mitochondrion biogenesis, and maize growth, Plant Cell 24 (2012) 676–691.
[34] J.L. Heazlewood, K.A. Howell, J. Whelan, A.H. Millar, Towards an analysis of the rice mitochondrial proteome, Plant Physiol. 132 (2003) 230–242.
[35] N.V. Lande, P. Subba, P. Barua, D. Gayen, T.K. Prasad, S. Chakraborty,

N. Chakraborty, Dissecting the chloroplast proteome of chickpea (Cicer arietinum L.) provides new insights into classical and non-classical functions, J. Proteome 165 (2017) 11–20.
[36] I.M. Møller, A.C. Lidén, I. Ericson, P. Gardeström, Isolation of submitochondrial particles with different polarities, Methods Enzymol. 148 (1987) 442–453.
[37] A. Vishwakarma, A. Kumari, L.A. Mur, K.J. Gupta, A discrete role for alternative oxidase under hypoxia to increase nitric oxide and drive energy production, Free Radic. Biol. Med. 122 (2018) 40–51.
[38] S. Pandey, A. Kumari, C. Bharadwaj, K.J. Gupta, Measurement of respiration and internal oxygen in germinating cicer arietinum L. seeds using optic microsensor, Plant Respiration and Internal Oxygen, Springer, 2017, pp. 57–62.
[39] K.-L. Chan, C.-L. Ho, P. Namasivayam, S. Napis, A simple and rapid method for RNA isolation from plant tissues with high phenolic compounds and polysaccharides, Protocol Exchange 184 (2007).
[40] R.E. Voorips, MapChart: Software for the graphical presentation of linkage maps and QTLs, J. Hered 93 (2002) 77–78.
[41] A. Pandey, M.K. Choudhary, D. Bhushan, A. Chattopadhyay, S. Chakraborty, A. Datta, N. Chakraborty, The nuclear proteome of chickpea (*Cicer arietinum* L.) reveals predicted and unexpected proteins, J. Proteome Res. 5 (2006) 3301–3311.
[42] D. Bhushan, A. Pandey, A. Chattopadhyay, M.K. Choudhary, S. Chakraborty, A. Datta, N. Chakraborty, Extracellular matrix proteome of chickpea (*Cicer a rietinum* L.) illustrates pathway abundance, novel protein functions and evolutionary perspect, J. Proteome Res. 5 (2006) 1711–1720.
[43] D. Bhushan, D.K. Jaiswal, D. Ray, D. Basu, A. Datta, S. Chakraborty, N. Chakraborty, Dehydration-responsive reversible and irreversible changes in the extracellular matrix: comparative proteomics of chickpea genotypes with contrasting tolerance, J. Proteome Res. 10 (2011) 2027–2046.
[44] P. Subba, R. Kumar, S. Gayali, S. Shekhar, S. Parveen, A. Pandey, A. Datta, S. Chakraborty, N. Chakraborty, Characterisation of the nuclear proteome of a dehydration-sensitive cultivar of chickpea and comparative proteomic analysis with a tolerant cultivar, Proteomics 13 (2013) 1973–1992.
[45] D.K. Jaiswal, P. Mishra, P. Subba, D. Rathi, S. Chakraborty, N. Chakraborty, Membrane-associated proteomics of chickpea identifies Sad1/UNC-84 protein (CaSUN1), a novel component of dehydration signaling, Sci. Rep. 4 (2014).
[46] P. Barua, P. Subba, N.V. Lande, K.K. Mangalaparthi, T.S.K. Prasad, S. Chakraborty, N. Chakraborty, Gel-based and gel-free search for plasma membrane proteins in chickpea (*Cicer arietinum* L.) augments the comprehensive data sets of membrane protein repertoire, J. Proteome 143 (2016) 199–208.
[47] J.L. Heazlewood, J.S. Tonti-Filippini, A.M. Gout, D.A. Day, J. Whelan, A.H. Millar, Experimental analysis of the Arabidopsis mitochondrial proteome highlights signaling and regulatory components, provides assessment of targeting prediction programs, and indicates plant-specific mitochondrial proteins, Plant Cell 16 (2004) 241–256.
[48] D. Ghosh, Z. Li, X.F. Tan, T.K. Lim, Y. Mao, Q. Lin, iTRAQ based quantitative proteomics approach validated the role of calcyclin binding protein (CacyBP) in promoting colorectal cancer metastasis, Mol. Cell. Proteomics 12 (2013) 1865–1880.
[49] C.S. Gan, P.K. Chong, T.K. Pham, P.C. Wright, Technical, experimental, and biological variations in isobaric tags for relative and absolute quantitation (iTRAQ), J. Proteome Res. 6 (2007) 821–827.
[50] Z. Wang, Q. Zhou, Y. Li, L. Qiao, Q. Pang, B. Huang, iTRAQ-based quantitative proteomic analysis of conidia and mycelium in the filamentous fungus Metarhizium robertsii, Fungal Biol. 122 (2018) 651–658.
[51] P. Subba, R. Kumar, S. Gayali, S. Shekhar, S. Parveen, A. Pandey, A. Datta, S. Chakraborty, N. Chakraborty, Characterisation of the nuclear proteome of a dehydration-sensitive cultivar of chickpea and comparative proteomic analysis with a tolerant cultivar, Proteomics 13 (2013) 1973–1992.
[52] M. Nuell, D. Stewart, L. Walker, V. Friedman, C. Wood, G. Owens, J. Smith, E. Schneider, R. Dell'Orco, C. Lumpkin, Prohibitin, an evolutionarily conserved intracellular protein that blocks DNA synthesis in normal fibroblasts and HeLa cells, Mol. Cell. Biol. 11 (1991) 1372–1381.
[53] S. Mishra, S.R. Ande, B. Nyomba, The role of prohibitin in cell signaling, The FEBS J. 277 (2010) 3937–3946.
[54] A. Takahashi, T. Kawasaki, H.L. Wong, U. Suharsono, H. Hirano, K. Shimamoto, Hyperphosphorylation of a mitochondrial protein, prohibitin, is induced by calyculin A in a rice lesion-mimic mutant cdr1, Plant Physiol. 132 (2003) 1861–1869.
[55] J.C. Chen, C.Z. Jiang, M.S. Reid, Silencing a prohibitin alters plant development and senescence, Plant J. 44 (2005) 16–24.
[56] C.S. Ahn, J.H. Lee, A. Reum Hwang, W.T. Kim, H.S. Pai, Prohibitin is involved in mitochondrial biogenesis in plants, Plant J. 46 (2006) 658–667.
[57] L.A. Kelley, S. Mezulis, C.M. Yates, M.N. Wass, M.J. Sternberg, The Phyre2 web portal for protein modeling, prediction and analysis, Nat. Protoc. 10 (2015) 845–858.
[58] V. Wardhan, K. Jahan, S. Gupta, S. Chennareddy, A. Datta, S. Chakraborty, N. Chakraborty, Overexpression of CaTLP1, a putative transcription factor in chickpea (*Cicer arietinum* L.), promotes stress tolerance, Plant Mol. Biol. 79 (2012) 479–493.
[59] J.K. Verma, S. Gayali, S. Dass, A. Kumar, S. Parveen, S. Chakraborty, N. Chakraborty, OsAlba1, a dehydration-responsive nuclear protein of rice (*Oryza sativa* L. ssp. indica), participates in stress adaptation, Phytochemistry 100 (2014) 16–25.
[60] S. Parveen, D.B. Gupta, S. Dass, A. Kumar, A. Pandey, S. Chakraborty, N. Chakraborty, Chickpea ferritin CaFer1 participates in oxidative stress response, and promotes growth and development, Sci. Rep. 6 (2016) 31218.
[61] H. Shinshi, Ethylene-regulated transcription and crosstalk with jasmonic acid, Plant Sci. 175 (2008) 18–23.
[62] K. Kazan, J.M. Manners, Jasmonate signaling: toward an integrated view, Plant Physiol. 146 (2008) 1459–1468.
[63] C.M. Pieterse, D. Van der Does, C. Zamioudis, A. Leon-Reyes, S.C. Van Wees, Hormonal modulation of plant immunity, Annu. Rev. Cell Dev. Biol. 28 (2012) 489–521.
[64] D. Bhushan, A. Pandey, M.K. Choudhary, A. Datta, S. Chakraborty, N. Chakraborty, Comparative proteomics analysis of differentially expressed proteins in chickpea extracellular matrix during dehydration stress, Mol.Cell. Proteomics 6 (2007) 1868–1884.
[65] A. Pandey, S. Chakraborty, A. Datta, N. Chakraborty, Proteomics approach to identify dehydration responsive nuclear proteins from chickpea (*Cicer arietinum* L.), Mol. Cell. Proteomics 7 (2008) 88–107.
[66] E.A. Bray, Plant responses to water deficit, Trends Plant Sci. 2 (1997) 48–54.
[67] M. Bonora, M.R. Wieckowski, C. Chinopoulos, O. Kepp, G. Kroemer, L. Galluzzi, P. Pinton, Molecular mechanisms of cell death: central implication of ATP synthase in mitochondrial permeability transition, Oncogene 34 (2015) 1475–1486.
[68] M.L.E. Galvis, S. Marttila, G. Håkansson, J. Forsberg, C. Knorpp, Heat stress response in pea involves interaction of mitochondrial nucleoside diphosphate kinase with a novel 86-kilodalton protein, Plant Physiol. 126 (2001) 69–77.
[69] G. Clark, D. Konopka-Postupolska, J. Hennig, S. Roux, Is annexin 1 a multifunctional protein during stress responses? Plant Signal. Behav. 5 (2010) 303–307.
[70] E.V. Doukhanina, S. Chen, E. van der Zalm, A. Godzik, J. Reed, M.B. Dickman, Identification and functional characterization of the BAG protein family in Arabidopsis thaliana, J. Biol. Chem. 281 (2006) 18793–18801.
[71] L. Bedford, S. Paine, P.W. Sheppard, R.J. Mayer, J. Roelofs, Assembly, structure, and function of the 26S proteasome, Trends Cell Biol. 20 (2010) 391–401.
[72] D. Bekh-Ochir, S. Shimada, A. Yamagami, S. Kanda, K. Ogawa, M. Nakazawa, M. Matsui, M. Sakuta, H. Osada, T. Asami, A novel mitochondrial DnaJ/Hsp40 family protein BIL2 promotes plant growth and resistance against environmental stress in brassinosteroid signaling, Planta 237 (2013) 1509–1525.
[73] X. Wang, X. Cai, C. Xu, Q. Wang, S. Dai, Drought-responsive mechanisms in plant leaves revealed by proteomics, Int. J. Mol. Sci. 17 (2016) 1706.
[74] L. Kang, Y.S. Wang, S.R. Uppalapati, K. Wang, Y. Tang, V. Vadapalli, B.J. Venables, K.D. Chapman, E.B. Blancaflor, K.S. Mysore, Overexpression of a fatty acid amide hydrolase compromises innate immunity in Arabidopsis, Plant J. 56 (2008) 336–349.
[75] G. Piro, M.R. Leucci, K. Waldron, G. Dalessandro, Exposure to water stress causes changes in the biosynthesis of cell wall polysaccharides in roots of wheat cultivars varying in drought tolerance, Plant Sci. 165 (2003) 559–569.
[76] T. Phung, H.-i. Jung, J. Park, J.-G. Kim, K. Back, S. Jung, Porphyrin biosynthesis control under water stress: sustained porphyrin status correlates with drought tolerance in transgenic rice, Plant Physiol. 157 (2011) 1746–1764.
[77] S. Franz, B. Ehlert, A. Liese, J. Kurth, A.-C. Cazalé, T. Romeis, Calcium-dependent protein kinase CPK21 functions in abiotic stress response in Arabidopsis thaliana, Mol. Plant 4 (2011) 83–96.
[78] A. Sugiura, S. Mattie, J. Prudent, H.M. McBride, Newly born peroxisomes are a hybrid of mitochondrial and ER-derived pre-peroxisomes, Nature 542 (2017) 251–254.
[79] R.J. Dimario, H. Clayton, A. Mukherjee, M. Ludwig, J.V. Moroney, Plant carbonic anhydrases: structures, locations, evolution, and physiological roles, Mol. Plant 10 (2017) 30–46.
[80] B. Williams, M. Kabbage, R. Britt, M.B. Dickman, AtBAG7, an Arabidopsis Bcl-2–associated athanogene, resides in the endoplasmic reticulum and is involved in the unfolded protein response, Proc. Natl. Acad. Sci. 107 (2010) 6088–6093.
[81] Y. Wang, W.-Z. Zhang, L.-F. Song, J.-J. Zou, Z. Su, W.-H. Wu, Transcriptome analyses show changes in gene expression to accompany pollen germination and tube growth in Arabidopsis, Plant Physiol. 148 (2008) 1201–1211.
[82] Y.-S. Choi, J.H. Jeong, H.-K. Min, H.-J. Jung, D. Hwang, S.-W. Lee, Y.K. Pak, Shotgun proteomic analysis of mitochondrial D-loop DNA binding proteins: identification of mitochondrial histones, Mol. BioSyst. 7 (2011) 1523–1536.
[83] J. Sun, C.H. Bird, H.H. Salem, P. Bird, Association of annexin V with mitochondria, FEBS Lett. 329 (1993) 79–83.
[84] D. Chevallier, R. Douce, Interactions between mitochondria and chloroplasts in cells: I. Action of cyanide and of 3-(3, 4-Dichlorophenyl)-1, 1-dimethylurea on the spore of funaria hygrometrica, Plant Physiol. 57 (1976) 400–402.
[85] K. Oikawa, S. Matsunaga, S. Mano, M. Kondo, K. Yamada, M. Hayashi, T. Kagawa, A. Kadota, W. Sakamoto, S. Higashi, Physical interaction between peroxisomes and chloroplasts elucidated by in situ laser analysis, Nature Plants 1 (2015) 15035.
[86] C. Osman, C. Merkwirth, T. Langer, Prohibitins and the functional compartmentalization of mitochondrial membranes, J. Cell Sci. 122 (2009) 3823–3830.